



저작자표시-비영리-변경금지 2.0 대한민국

이용자는 아래의 조건을 따르는 경우에 한하여 자유롭게

- 이 저작물을 복제, 배포, 전송, 전시, 공연 및 방송할 수 있습니다.

다음과 같은 조건을 따라야 합니다:



저작자표시. 귀하는 원저작자를 표시하여야 합니다.



비영리. 귀하는 이 저작물을 영리 목적으로 이용할 수 없습니다.



변경금지. 귀하는 이 저작물을 개작, 변형 또는 가공할 수 없습니다.

- 귀하는, 이 저작물의 재이용이나 배포의 경우, 이 저작물에 적용된 이용허락조건을 명확하게 나타내어야 합니다.
- 저작권자로부터 별도의 허가를 받으면 이러한 조건들은 적용되지 않습니다.

저작권법에 따른 이용자의 권리는 위의 내용에 의하여 영향을 받지 않습니다.

이것은 [이용허락규약\(Legal Code\)](#)을 이해하기 쉽게 요약한 것입니다.

[Disclaimer](#)

공학석사학위논문

**Prototype Development of a Deployable  
Measurement System for Civil  
Infrastructures**

설치 편의형 인프라 시설물

계측 시스템 개발

2019년 8월

서울대학교 대학원

건설환경공학부

김 태 훈



## **ABSTRACT**

Although the science of theoretical fluid mechanics has been well developed and the computational methods are rapidly advancing, the measurement of the wind-induced pressure and vibration of civil infrastructures, such as long-span bridges, high-rise buildings, wind barriers, etc., is essential to understand the structural performance of the infrastructure.

The conventional measurement system requires many devices such as a power source, a data acquisition device, sensors, cables, etc., which pose difficulty in installation and measurement on bridges or buildings that are in use. Therefore, it is necessary to develop a miniaturized device so that researchers and engineers can easily obtain wind-induced pressure and vibration data at any desired locations without interrupting the use of the infrastructure.

This paper proposes a prototype development which can measure wind pressure acting on a structure and acceleration of the structure. In this study, micro-electronic-mechanical-system (MEMS) sensors are used in the prototype device such as acceleration and pressure sensors. It is expected that the successful development of the sensor module will help engineers and researchers measure wind pressure acting on a structure and associated structural vibration.

**Keywords: Data acquisition system, MEMS sensor, Structural vibration,  
Wireless sensor, GPS base time synchronization**

**Student Number: 2017-27232**

# TABLE OF CONTENTS

ABSTRACT.....	I
TABLE OF CONTENTS .....	III
LIST OF FIGURES .....	V
LIST OF TABLES .....	VII
CHAPTER 1 .....	1
INTRODUCTION .....	1
1.1 RESEARCH BACKGROUND.....	1
1.2 PREVIOUS WORK AND PROBLEM DEFINITION.....	3
1.3 ISSUES OF COMMERCIAL WIRELESS SENSOR.....	3
1.4 ISSUES OF DESIGNED WIRELESS SENSOR .....	4
1.5 PROTOTYPE OF DEPLOYABLE MEASUREMENT DEVICE .....	5
CHAPTER 2 .....	7
TIME SYNCHRONIZATION.....	7
2.1 MICRO CONTROL UNIT (MCU) CLOCK.....	7
2.2 REAL TIME CLOCK (RTC) .....	8
2.3 GLOBAL POSITIONING SYSTEM (GPS).....	10
CHAPTER 3 .....	13

ACCELEROMETER .....	13
3.1 TYPE OF ACCELEROMETER.....	13
3.1.1 Piezo electric type accelerometer .....	13
3.1.2 Capacitive type accelerometer.....	14
3.2 ACCELEROMETER VALIDATION TEST .....	15
3.2.1 Sinusoidal motion.....	16
3.2.2 Seismic motion .....	19
3.3 APPLICATION OF PROPOSED DEVICE.....	20
3.3.1 Suspended footbridge .....	21
CHAPTER 4 .....	34
PRESSURE SENSOR .....	34
4.1 TYPE OF PRESSURE SENSOR .....	34
4.1.1 Piezo-resistive type pressure sensor .....	34
4.2 PRESSURE SENSOR VALIDATION TEST.....	35
4.2.1 Pressure change test according to volume change in closed cylinder .....	35
4.2.2 Pressure change test according to wind speed in wind tunnel test .....	37
CHAPTER 5 .....	42
SUMMARY AND CONCLUSIONS.....	42
REFERENCES .....	44

## LIST OF FIGURES

FIG 1.1. ACCELEROMETER LAYOUT OF SEO-HAE BRIDGE .....	1
FIG 1.2. CONVENTIONAL MEASUREMENT SYSTEM .....	2
FIG 1.3. TIME DRIFT ISSUE IN COMMERCIAL WIRELESS SENSOR .....	4
FIG 1.4. DATA MISSING ISSUE DURING DATA TRANSMISSION .....	4
FIG 1.5. THE COMPONENTS OF THE PROPOSED DEVICE .....	5
FIG.2. 1. DIFFERENCE OF TIME ACCORDING TO TIME COUNTING METHOD.....	9
FIG.2. 2. GPS SIGNAL TRANSMISSION WHEREVER UNDER CLEAR SKY .....	11
FIG.2. 3. OPERATION FLOW OF THE PROPOSED DEVICE .....	11
FIG. 3. 1 PRINCIPLE OF PIEZOELECTRIC TYPE ACCELEROMETER.....	14
FIG. 3. 2 PRINCIPLE OF CAPACITIVE TYPE ACCELEROMETER .....	14
FIG. 3. 3. SHAKING TABLE: QUANSER's SHAKER2.....	16
FIG. 3. 4. ACCELERATION DATA IN 2HZ SINUSOIDAL MOTION.....	17
FIG. 3. 5. ACCELERATION FFT RESULTS OF EACH FREQUENCY MOTION .....	18
FIG. 3. 6. ACCELERATION DATA IN SEISMIC MOTION.....	20
FIG. 3. 7. GEO-CHANGE SUSPENDED FOOTBRIDGE .....	21
FIG. 3. 8. ACCELEROMETER LAYOUT OF GEO-CHANGE SUSPENDED FOOTBRIDGE .....	22
FIG. 3. 9. LOCATION OF VERTICAL IMPACT .....	22
FIG. 3. 10. MEASURED ACCELERATIONS AT THE 1 <sup>ST</sup> SPAN CENTER .....	23
FIG. 3. 11. ACCELERATION FFT RESULTS OF 1 <sup>ST</sup> SPAN.....	24
FIG. 3. 12. MEASURED ACCELERATIONS AT THE 3 <sup>RD</sup> SPAN CENTER.....	25
FIG. 3. 13. ACCELERATION FFT RESULTS OF 3 <sup>RD</sup> SPAN.....	26
FIG. 3. 14. ISO WEIGHTING CURVE ACCORDING TO FREQUENCY RANGE .....	27



FIG. 3. 15. LOCATION OF ACCELERATION MEASURING POINT .....	29
FIG. 3. 16. . LOCATIONS OF THE EXPANSION JOINTS ON THE BRIDGE .....	30
FIG. 3. 17. VERTICAL ACCELERATION OF THE VEHICLE RUNNING AT 100 KM/H .....	31
FIG. 3. 18. 3-AXIS OF MEASURED ACCELERATION AT 100KM/H.....	32
FIG. 3. 19. TOTAL RESPONSE ACCELERATION BASED ON ISO .....	32
FIG 4.1. PRINCIPLE OF PIEZO-RESISTIVE TYPE PRESSURE SENSOR .....	35
FIG 4.2. BASIC CONCEPT: BOYLE’S LAW .....	36
FIG 4.3. SETUP OF PRESSURE VALIDATION TEST USING SHAKING TABLE .....	36
FIG 4.4. MEASURED PRESSURE DATA THROUGH BMP280.....	37
FIG 4.5. WIND TUNNEL IN SEOUL NATIONAL UNIVERSITY .....	38
FIG 4.6. SETUP OF PRESSURE SENSOR VALIDATION TEST USING WIND TUNNEL .....	38
FIG 4.7. MEASURING POINT OF SOUND BARRIER MODEL.....	39
FIG 4.8. MEASURED PRESSURE WHICH ACTING ON THE SOUND BARRIER ACCORDING TO WIND SPEED.....	40
FIG 4.9. CORRELATION BETWEEN NETSCANNER9116 AND MPU6050.....	40

## LIST OF TABLES

TABLE.3. 1. DIFFERENCES OF 1ST SPAN FFT RESULTS BETWEEN TWO ACCELERATIONS .....	24
TABLE.3. 2. DIFFERENCES OF 3 <sup>RD</sup> SPAN FFT RESULTS BETWEEN TWO ACCELERATIONS .....	26
TABLE.3. 3. WEIGHTING FACTOR ACCORDING TO ACCELEROMETER LOCATION AND DIRECTION .....	28
TABLE.3. 4. APPROXIMATE INDICATIONS OF REACTIONS.....	28

# CHAPTER 1

## INTRODUCTION

### 1.1 Research background

Although theoretical hydrodynamics have been developed continuously and computational methods have been developed rapidly, analyze the dynamic characteristics of civil infrastructures by measuring the actual structural vibration is essential to prevent the large vibrations owing to external forces such as wind load, vehicle load.

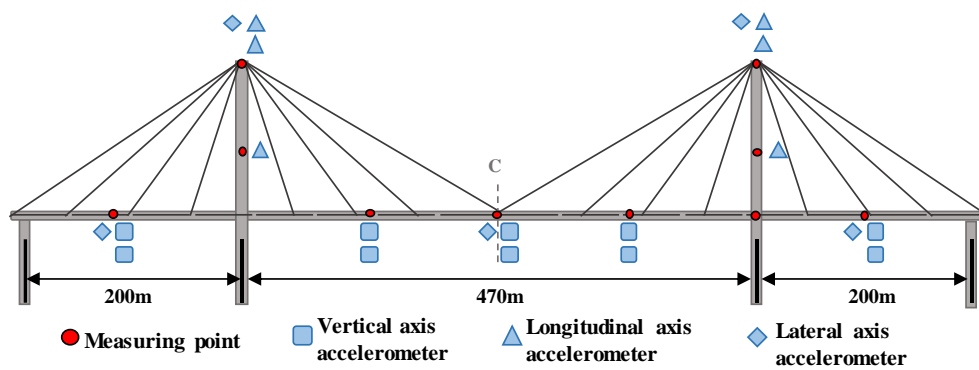
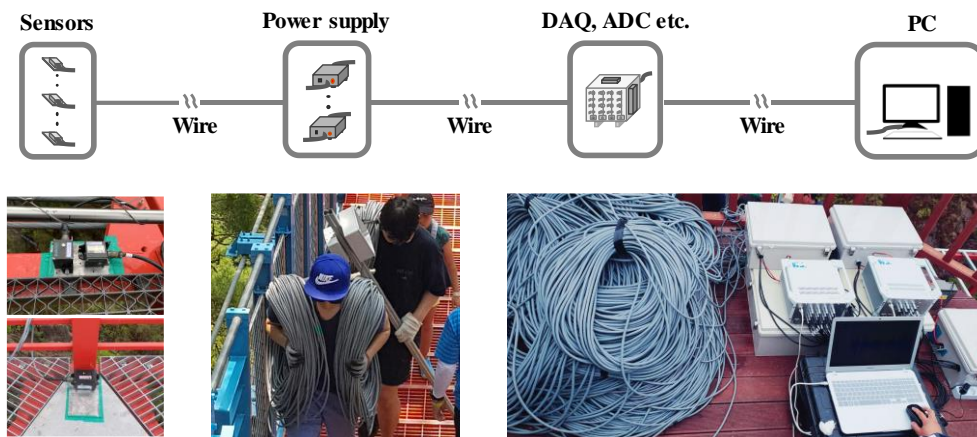


Fig 1.1. Accelerometer layout of Seo-hae bridge

However, the conventional measurement system requires a lot of equipment

such as a power generator, a central process device, a data storage device, and sensors, and each device have to be connected by a long cable. In addition, it is difficult for researchers to compose their own measurement system and install a sensor on a civil infrastructure due to the high initial cost and difficulty of wired sensor installation. Because of these problems, researchers can not directly obtain needed data and can evaluate the structure characteristic based on data that doesn't meet their purpose.



**Fig 1.2. Conventional measurement system**

In this study, propose a deployable measurement system which the researchers can easily measure the vibrations of the structures and this system will be helpful to analyze the dynamic characteristics of the civil infrastructures through the properly measured data.

## 1.2 Previous work and problem definition

In the measurement field, many wireless measurement systems are being used to quickly and easily measure the structural vibration. There are two main types of wireless sensors that are already being used. One is a commercial wireless sensor made by mechanical engineering majors not only for structures but also for vehicles and human movements, etc. and the other is a wireless sensor network developed directly by civil engineering researchers with the aim of measuring civil structures.

## 1.3 Issues of commercial wireless sensor

In the case of commercial wireless sensors, since they are already commercialized, the size of the sensor is small and the appearance of the sensor is well finished. In addition, many proprietary programs have been developed, so the user can easily operate the sensor through the manual. However, the price of commercial wireless sensors is several times more expensive than conventional sensor, which is not suitable for multi-point measurement, and the performance of sensors (Resolution, Noise, Measurement range, etc.) cannot be selected for the purpose and may have to purchase the high-performance sensors that are not required but for meeting a particular performance at a high price. The commercial wireless

sensor. Commercial wireless sensor can measure the data without a central control device such as a computer because it works independently through their own internal controller. However, because there is no central control device, it is impossible to update the time periodically, so that the time of each commercial wireless device can be different or time drifting may occur.

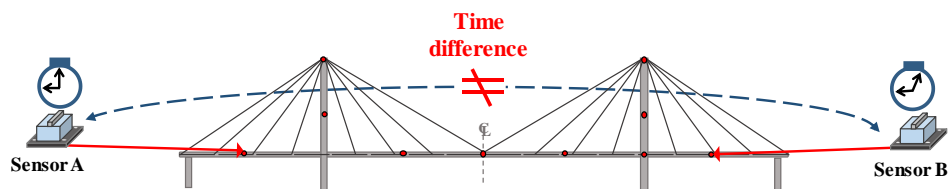


**Fig 1.3. Time drift issue in commercial wireless sensor**

#### 1.4 Issues of designed wireless sensor

The use of well designed wireless sensor system by civil engineer also has issues for general civil engineers. There are several research groups about Wireless Sensor Networks(WSNs) such as Imote2 for the Structural Health Monitoring (SHM). These devices are useful and powerful for civil engineers but since these are not mass-produced, these are difficult to obtain compared to commercial device. In addition, since these devices are built with high-level technology, the user requires knowledge about sensing technique to handle the unusual situation.

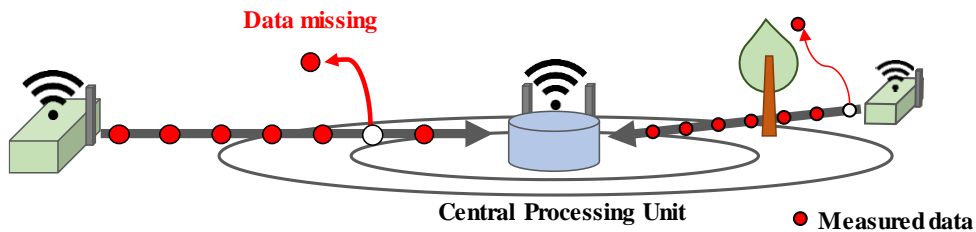


**Fig 1.4. Data missing issue during data transmission**

## 1.5 Prototype of deployable measurement device

This research the proposed a device to solve the problem of conventional wireless sensor which is not time-synchronized and too expensive for multi-point measurement. The proposed device consists of MCU (ATmega328P) and GPS (Ultimate GPS), Accelerometer (MPU6050), Pressure sensor (BMP280) and Micro SD. All components of the proposed device are small and lightweight, easy to carry and install. Moreover, the components are mass-produced so easy to purchase and inexpensive. If this research is successfully developed, it is expected that researchers easily obtain the desired data.

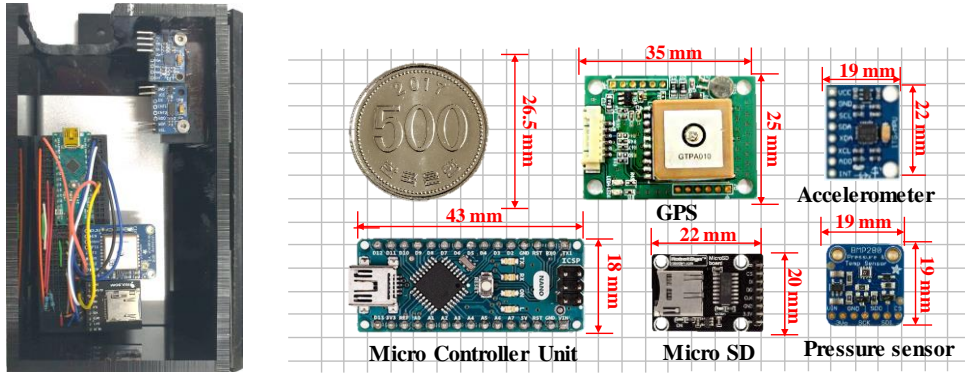


**Fig 1.5. The components of the proposed device**



## **CHAPTER 2**

### **Time synchronization**

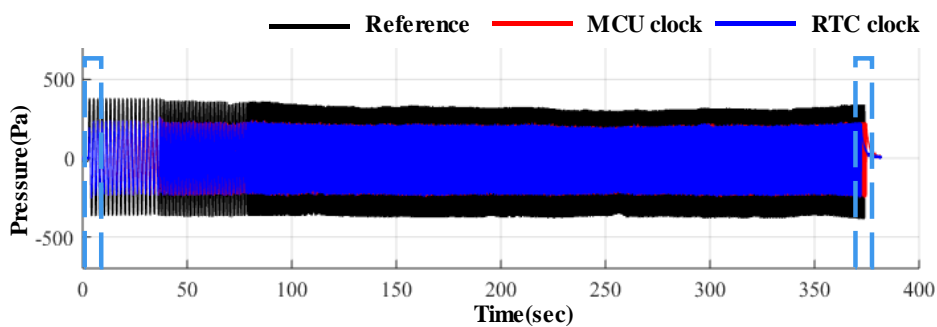
#### **2.1 Micro Control Unit (MCU) clock**

The simplest way to compare MCU performance is to compare the MCU clock speed. MCU clock speed is not only representing the processing speed of the MCU but also affects the setting of the internal timer, ADC, I2C, etc. of the MCU function which needs the clock. Therefore, it is important to select the MCU having the clock speed suitable for the purpose. The MCU used in the proposed device is ATmega328P which is widely used in many fields and it has 16MHz clock speed.

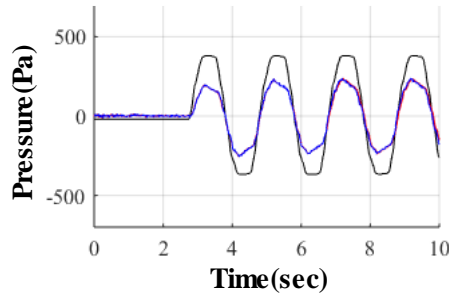
The timer function using the MCU clock is used to detect how much time has elapsed since the power was turned on, or to detect an elapsed time such as executing another task after a certain time. However, detecting an elapsed time through the MCU clock has several problems. When using the MCU clock for a long time, clock speed error can occur due to temperature change of MCU crystal and counter missing due to priority command which higher than the timer function. Therefore, it is not appropriate for use to make precise time stamp. Moreover, it is impossible to synchronize multiple devices using the MCU clock because the timer is reset when the MCU is not powered.

## 2.2 Real Time Clock (RTC)

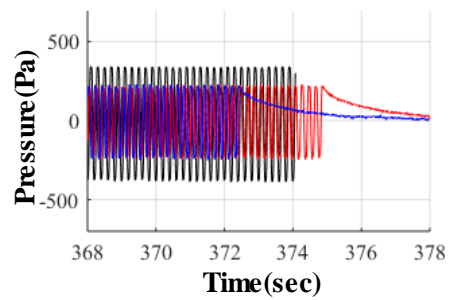
Like MCU clock, RTC is a computer clock that maintains the current time through counting vibration of internal crystal and is used not only in measurement device but also in many places such as computers and digital watches. But the difference with the MCU clock is that RTC has a separate power source from a control device, the time stamp is maintained even if the central processing unit is turned off. Because RTC is designed to maintain time, it can maintain time more accurately than the MCU Clock, and it can reduce power consumption rather than using MCU Clock. However, since the smallest unit of RTC count is seconds, it is not suitable for use for measurement device which stores more than 100 times per second. In addition, as same with MCU clocks issue, RTC also has time drift issue due to temperature changes in crystal.



(a)



(b)



(c)

**Fig.2. 0-1. Difference of time according to time counting method**

Figure2.1 shows the pressure value when the volume of the closed cylinder is periodically changed, each line has the different time stamp measured by the MCU clock and the RTC clock, the actual elapsed time. At the beginning of the measurement, all three lines show the same phase but at the end of the measurement, the phases are change. As confirmed from the Fig., If the reference time is dependent on the internal controller, time drift may be caused by various reason. Therefore, periodic time update is required through the external reference time.

## 2.3 Global Positioning System (GPS)

The GPS receiver receives signals transmitted from three or more GPS satellites to determine the position of the satellites and receivers through the signal arrival time difference, and synchronizes the respective times through the transmitted time information. The proposed device synchronizes the time with other devices through the two types of GPS signal. The first signal is the National Marine Electronics Association (NMEA) which has a relatively long data length signal to contain information such as time, position orientation, and so on. Through the NMEA signal, it is possible to receive global time from the maximum year unit to the minimum centi-second unit, so that the time stamp of the proposed device can be synchronized even if each device operates at different time. The other is a very accurate pulse signal with a one-second period called Pulse-Per-Second (PPS). Since the length of the NMEA signal is long, there is a little arrival time error until the signal is transmitted to each device in the satellite. However, since the PPS signal is just a simple pulse signal, the signal length is short and arrival time to devices is very accurate.

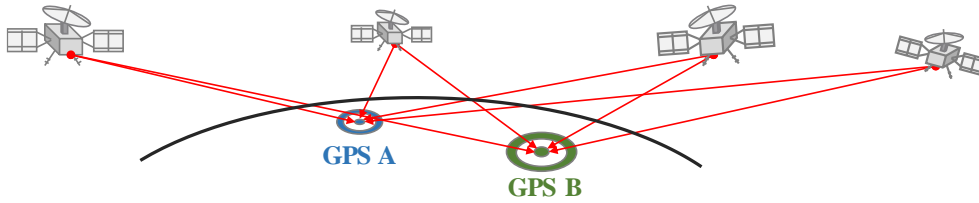


**Fig.2. 0-2. GPS signal transmission wherever under clear sky**

The proposed device operates in order of time array part and measuring part after power is connected. Since the NMEA signal has a lot of information including the global time, the signal length is too long and the measurement signal can not be read through the sensor while the NMEA signal is received, so the operation section is divided as two parts. For this reason, the Time array part does not read the sensor data and only receive NMEA and PPS to make the global time stamp. After the time array part, the Measuring part does not receive the NMEA but only receives the PPS signal, keeps the time stamp, and simultaneously reads the measured data through the sensor.

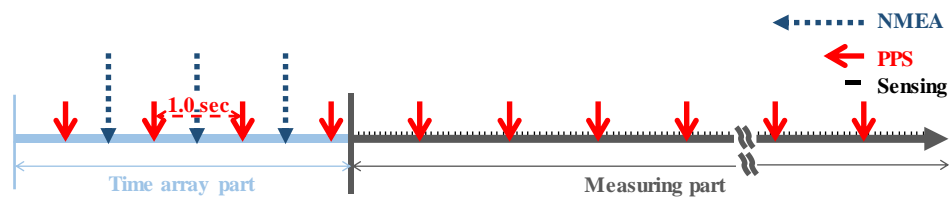


**Fig.2. 0-3. Operation flow of the proposed device**

The proposed sensor updates the reference time periodically through the GPS

attached to each device, and can independently generate a time stamp synchronized with the global time without an additional central control device. It is also possible to synchronize with another device that uses global time without additional devices.

## **CHAPTER 3**

### **Accelerometer**

Since the accelerometer uses various field not only civil engineering but also mechanical vibration, human motion, etc., so it is important to select an appropriate accelerometer according to the measurement purpose.

#### **3.1 Type of accelerometer**

Accelerometers are divided into two types depending on the measurement method: a piezo accelerometer and a capacitive accelerometer. Since the measurement frequency range and the maximum acceleration magnitude vary depending on the measurement principle, it is necessary to know about the measurement type of accelerometer.

##### **3.1.1 Piezo electric type accelerometer**

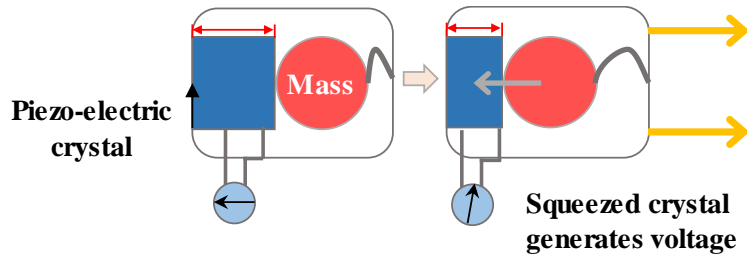


**Fig. 3. 1 Principle of piezoelectric type accelerometer**

Piezoelectric type accelerometers measure the acceleration using a piezoelectric effect that generates electric charges on the crystal surface due to internal polarization when a crystal such as barium oxide ( $\text{BaTiO}_3$ ) is subjected to a force. Piezoelectric type accelerometers have built-in amplification circuits (ICP, IIEEE), which can make low output impedance and it can make using long output cable. In addition, since the piezoelectric type has a linear response at high frequency, it is widely used for measuring high-frequency motion, and also the sensitivity of the sensor can be adjusted focused on a low frequency.

### 3.1.2 Capacitive type accelerometer

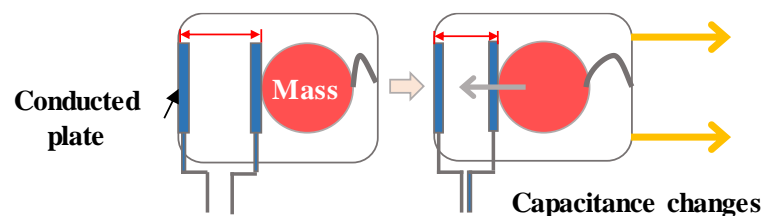


**Fig. 3. 2 Principle of capacitive type accelerometer**



The capacitive type accelerometer is an accelerometer widely used in the low-frequency range where the response is slow, such as the vibration of the structure. The vibration is measured using the effect that the capacitance changes according to displacement change between the two conducted plates. Capacitors, the main material used in capacitive type accelerometers are less affected to temperature changes, so It can be used in environments where the temperature changes greatly.

### 3.2 Accelerometer validation test

Before measuring actual structural vibration through the proposed device, experiments were conducted to verify the performance of MEMS accelerometers in a controlled environment. Accelerometer validation tests were carried out using QUANSER's Shaker 2 which 1axis screw motor type shaking table. Shaker 2 can simulate sinusoidal motion at specific single frequencies from 0.1 Hz to 5.0 Hz, and also it can simulate seismic motion which has various frequency components such as El-Centro.

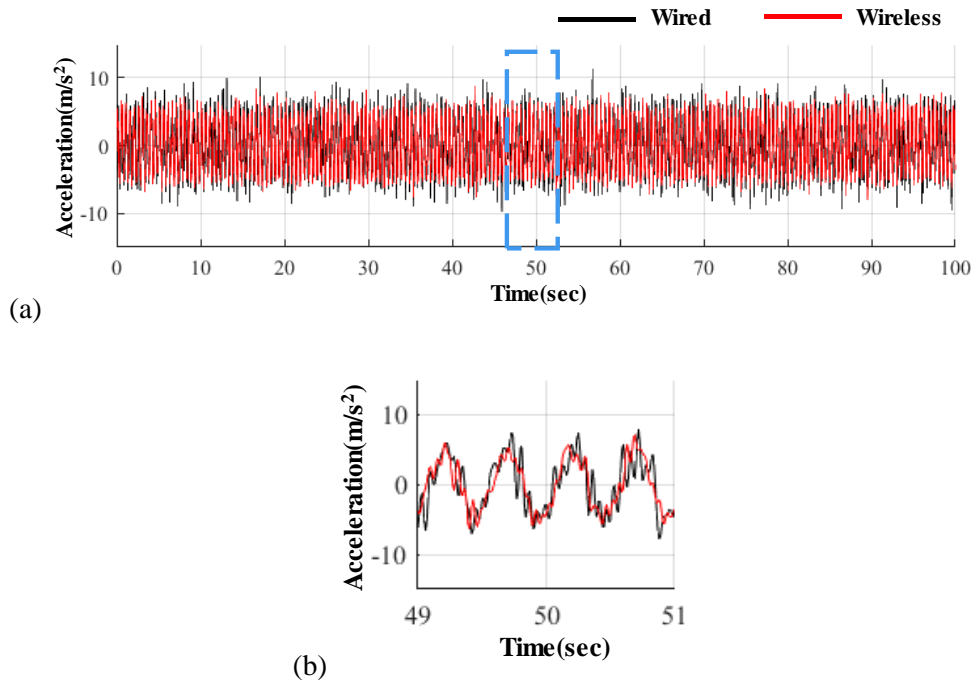


**Fig. 3.3. Shaking table: QUANSER's Shaker2**

Through these two types of indoor experiments, the measurable frequency range and the acceleration magnitude of the MEMS acceleration sensor were confirmed. The reference accelerometer used in the experiment is Kistler's 8315A single-axis analog output accelerometer. It has 2,000mV / g of sensitivity, 0Hz to 250Hz of frequency range, and 0.35mg resolution. The MEMS accelerometer used in the proposed device is InvenSense's MPU6050 3-axis digital accelerometer. It has 16,384 LSB/g of sensitivity and 16-bit analog to digital converter. Both accelerometers used in the experiments are Piezo-electric type accelerometers and can measure  $\pm 2.0g$  measurement range.

### 3.2.1 Sinusoidal motion

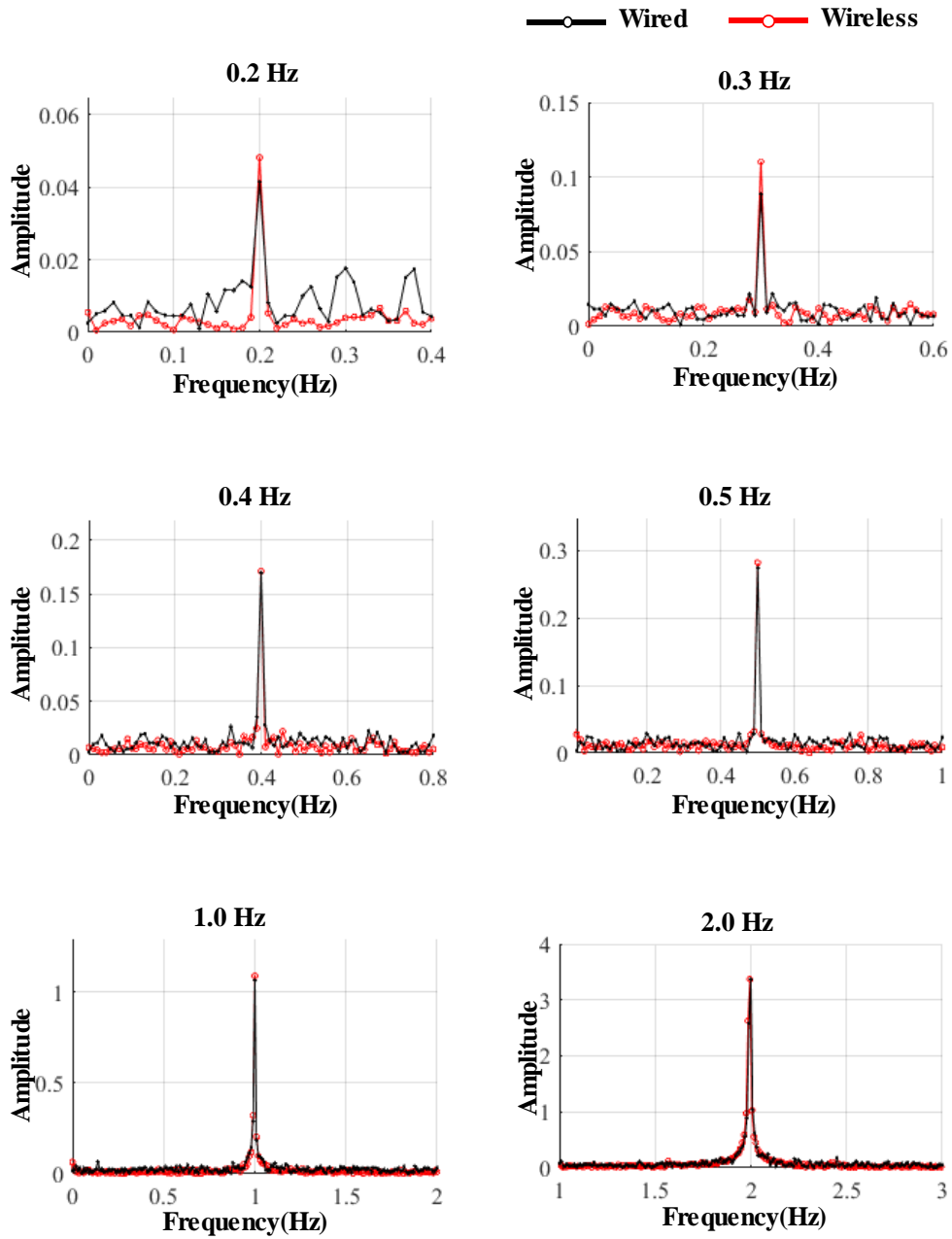
The sinusoidal motion tests were performed by simulating a single motion from 0.2 Hz to 2.0 Hz, which is the interested frequency range of civil infrastructure, and the acceleration was measured during 100 seconds for each frequency motion.



**Fig. 3. 4. Acceleration data in 2Hz sinusoidal motion**

Fig.3.4 shows the measured acceleration data through each accelerometer at 2Hz motion in the time domain. And the above graph shows that the 8315A and MPU6050 measure the same acceleration feature in magnitude and phase but the Fig3.4(b) graph also shows that the MPU6050 is less sensitive than 8315A in measuring small-high frequency vibrations occurred by screw motors.

In order to confirm both accelerometers measure the same frequency according to the motion frequency change, conduct the FFT to show the main frequency of measured acceleration. Fig.3.5 shows the FFT results of the measured data from 0.2Hz to 2.0Hz frequency range through the 8315A and MPU6050.

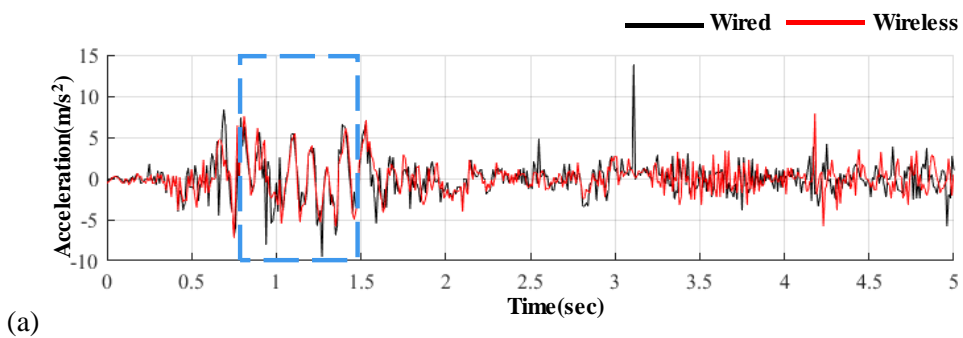


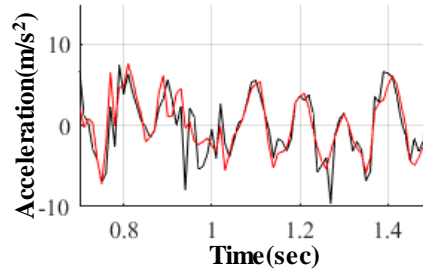
**Fig. 3. 5. Acceleration FFT results of each frequency motion**

Fig.3.5 shows that the acceleration measured at high-frequency motions have a more distinct peak compared to low-frequency motions and unexpectedly, Fig3.5 shows that the peak in the low-frequency motions is more pronounced on the MPU6050 than on the 8315A. Through the sinusoidal motion test, it is confirmed that the proposed device can measure the mode frequency of the actual structure.

### 3.2.2 Seismic motion

The second experiment was carried out to compare the accelerations obtained by measuring seismic motions which have various frequencies through two accelerometers. An El-Centro earthquake was used for the seismic motion test. Fig.3.6 shows the measured accelerations through 8315A and MPU6050 in time domain.





(b)

**Fig. 3. 6. Acceleration data in seismic motion**

Compared to the two measured accelerations, the magnitude and phase of both accelerations are similar overall, but the 8315A more sensitively measured small and high-frequency motion than MPU6050.

The results of the two validation tests showed that the acceleration measured from the proposed device is similar to the conventional wired accelerometer in magnitude and phase but it is confirmed that the proposed device is less sensitive than the conventional wired accelerometer in measuring small high-frequency motion.

### 3.3 Application of proposed device

It is confirmed that the proposed device can measure the interested frequency range of the structure (0Hz ~ 2Hz) through the validation tests. But before applying to the actual structure which has small vibration, another field test was carried out

on actual structure which have large vibrations to verify that the proposed sensor can be used to measure the dynamic characteristics of structures.

### 3.3.1 Suspended footbridge

The suspended footbridge is only supported by the steel cables without support structure such as pylons and piers, so it is easy to occur large vibration even in small impact. The footbridge used in the field test is a Geo-chang suspended footbridge located in Geo-chang, Korea, and it is composed of three different lengths of spans.

The proposed device and the wire accelerometer were attached to the same position of the footbridge and measured the bridge's vibration. The first one is Kinemetrics's ES-U2 which is 1-axis analog wired accelerometer and its measurement range is  $\pm 2.0g$ . The other is the MPU6050 3-axis wireless accelerometer used in the proposed device and its measurement range is set to  $\pm 2.0g$ .



**Fig. 3. 7. Geo-change suspended footbridge**

The two kind accelerometers were installed at the middle of the 1<sup>st</sup> span and 3<sup>rd</sup> span of the bridge, and a total of 400 kilograms of people jumped in place at the center of 1<sup>st</sup> span for simulating vertical impact.

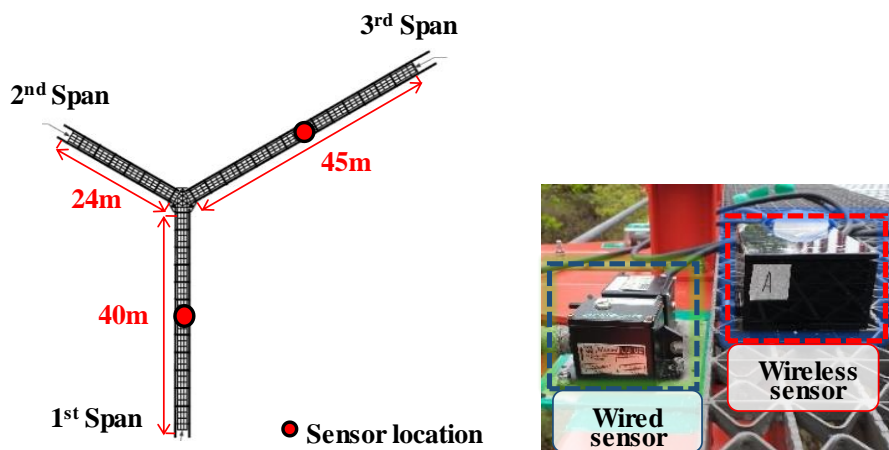


Fig. 3. 8. Accelerometer layout of Geo-change suspended footbridge

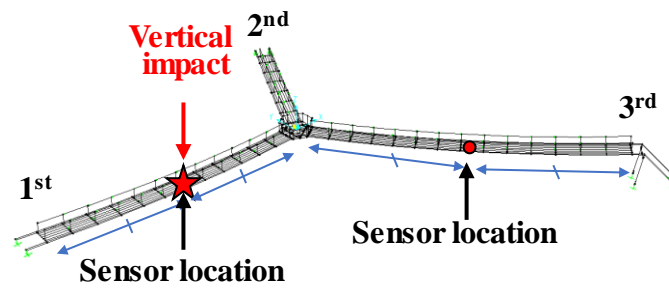
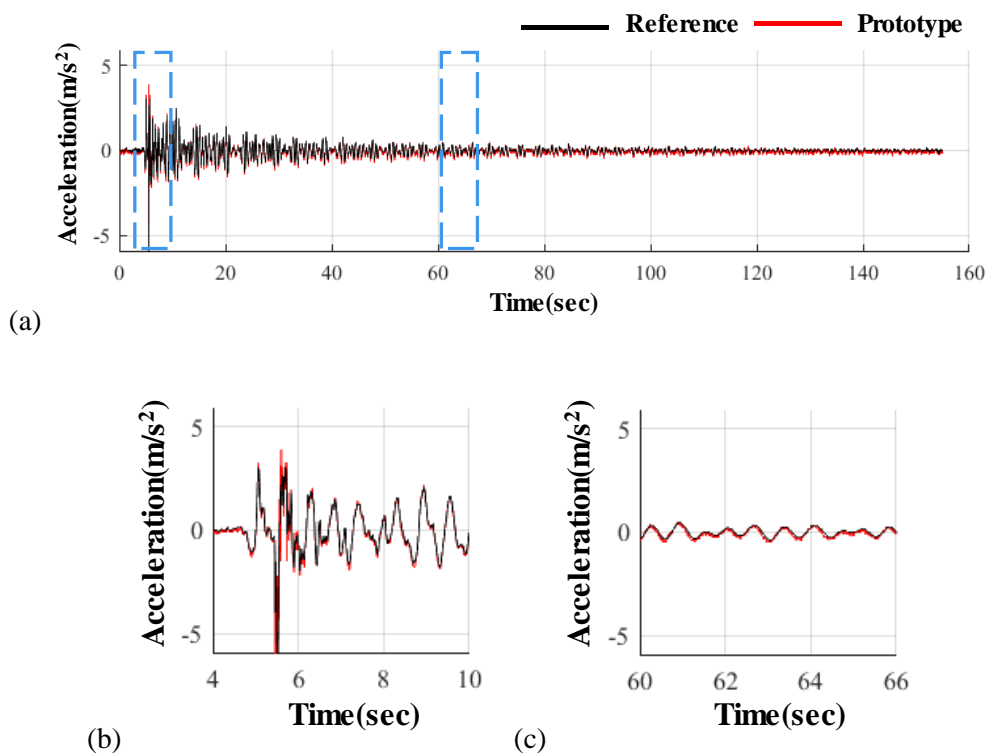


Fig. 3. 9. Location of vertical impact

Fig.3.10 shows the vertical acceleration data in time domain measured by ES-U2



wired accelerometer and MPU6050 at the center of 1<sup>st</sup> span. When the two accelerations measured at the 1<sup>st</sup> span of the loaded bridge were compared, it was confirmed that the acceleration magnitude and phase changes of both data were the same, and also time drift was not founded.



**Fig. 3. 10. Measured accelerations at the 1<sup>st</sup> span center**

Fig.3.11 is the vertical acceleration data in frequency domain measured by ES-U2 wired accelerometer and MPU6050 at the center of 1<sup>st</sup> span. Fig.3.11 shows that the frequency domain results of both measured accelerations are almost the same, and the maximum error of the peak is 1.308%.

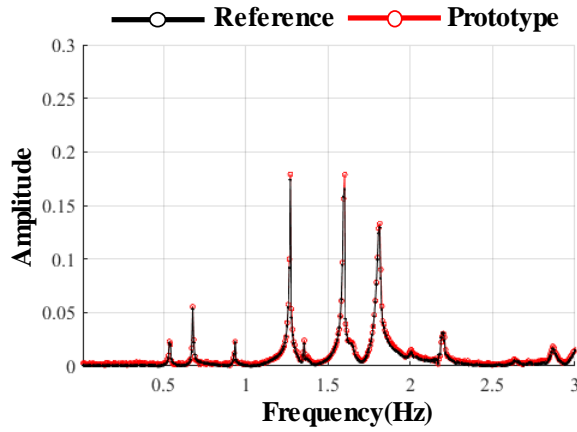
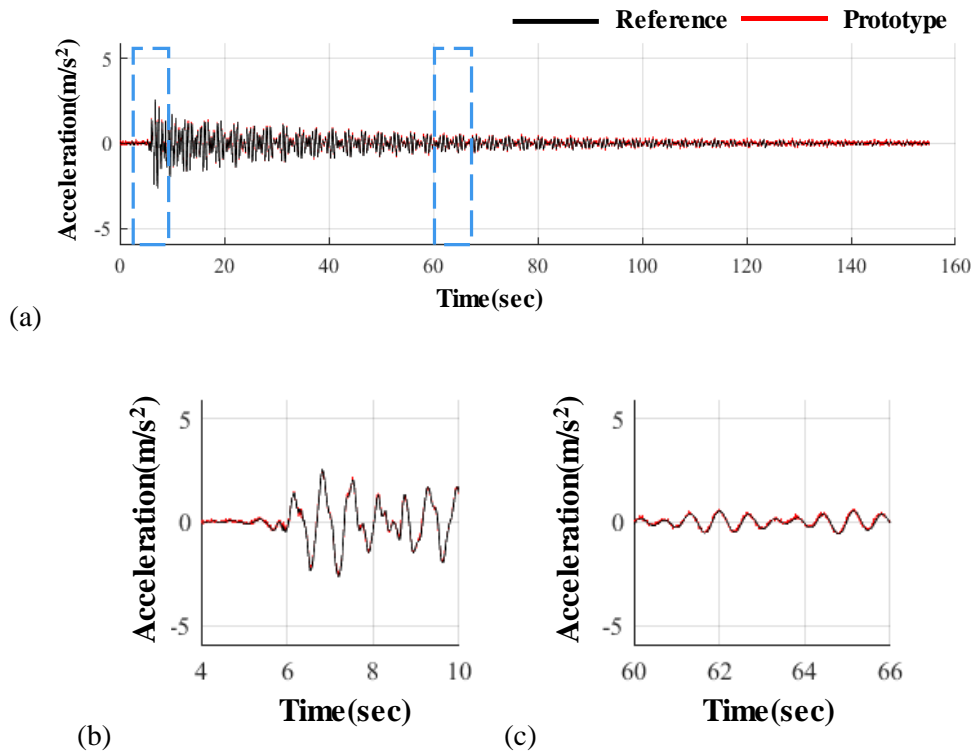


**Fig. 3. 11. Acceleration FFT results of 1st span**

**Table.3. 1. Differences of 1st span FFT results between two accelerations**

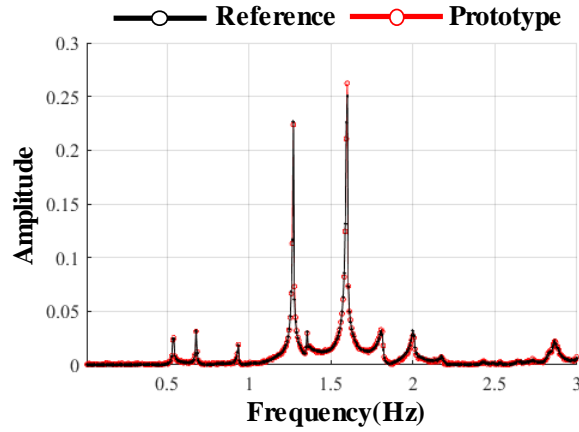
<b>Peaks</b>	<b>1<sup>st</sup></b>	<b>2<sup>nd</sup></b>	<b>3<sup>rd</sup></b>	<b>4<sup>th</sup></b>	<b>5<sup>th</sup></b>	<b>6<sup>th</sup></b>
Reference (Hz)	0.535	0.677	0.935	1.271	1.355	1.600
Prototype (Hz)	0.542	0.677	0.935	1.270	1.354	1.599
Difference (%)	1.308	0.000	0.000	0.079	0.074	0.063

Fig.3.12 shows the vertical acceleration data in time domain measured by ES-U2 wired accelerometer and MPU6050 at the center of 3<sup>rd</sup> span. When the two accelerations measured at the 3<sup>rd</sup> span of the loaded bridge were compared, it was confirmed that the acceleration magnitude and phase changes of both data were the same, and also time drift was not founded.



**Fig. 3. 12. Measured accelerations at the 3<sup>rd</sup> span center**

Fig.3.13 is the vertical acceleration data in frequency domain measured by ES-U2 wired accelerometer and MPU6050 at the center of 3<sup>rd</sup> span. Fig.3.13 shows that the frequency domain results of both measured accelerations are almost the same, and the maximum error of the peak is 0.836%.



**Fig. 3. 13. Acceleration FFT results of 3<sup>rd</sup> span**

**Table.3. 2. Differences of 3<sup>rd</sup> span FFT results between two accelerations**

<b>Peaks</b>	<b>1<sup>st</sup></b>	<b>2<sup>nd</sup></b>	<b>3<sup>rd</sup></b>	<b>4<sup>th</sup></b>	<b>5<sup>th</sup></b>	<b>6<sup>th</sup></b>
Reference (Hz)	0.535	0.677	0.935	1.271	1.355	1.600
Prototype (Hz)	0.536	0.678	0.936	1.270	1.355	1.160
Difference (%)	0.040	0.836	0.032	0.000	0.078	0.063

### 3.3.2 Vehicle serviceability

Considering the serviceability of using infrastructure is also an important part of the design of the structure. Since most structures are used not only by pedestrians but also by various means of transportation, so many factors such as the weight of the transportations, the vehicle speed, and the road surface condition have to be considered. In recent years, transportation analysis programs (CarSim, TruckSim, etc) have been developed for modeling the evaluating use serviceability. However,

it is quite difficult to accurately apply the state of actual structures to the program model, so the actual driving state should be measured and evaluated the serviceability numerically. In order to evaluate the serviceability of a vehicle running on the structure, the International Organization for Standardization (ISO) uses an acceleration data. In order to verify the using versatility of the proposed device, evaluated the serviceability of the bridge through the vehicle running.

ISO evaluates the inconvenience of the human body by multiplying the measured acceleration by the weight according to the position of the accelerometer, the vibration direction, and the frequency range of vibration. In the evaluation index below, ISO evaluates large discomfort in the vertical direction vibration and specific frequency range (less than 5 Hz) vibration.

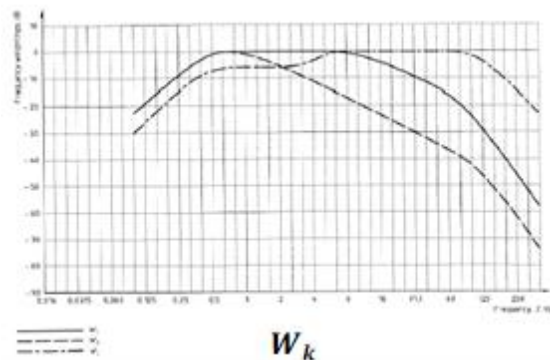


**Fig. 3. 14. ISO weighting curve according to frequency range**

**Table.3. 3. Weighting factor according to accelerometer location and direction**

<b>Location</b>	<b>Direction</b>	<b>Weighting</b>	<b>Multiplying factor(<i>k</i>)</b>
Floor	Fore-and-aft	$W_k$	0.25
Floor	Lateral	$W_k$	0.25
Floor	Vertical	$W_k$	0.40

The total response acceleration ( $a_v$ ) is calculated from the above coefficient factors and the serviceability is evaluated by the magnitude of  $a_v$ .

$$a_w = W \times a \quad (3.1)$$

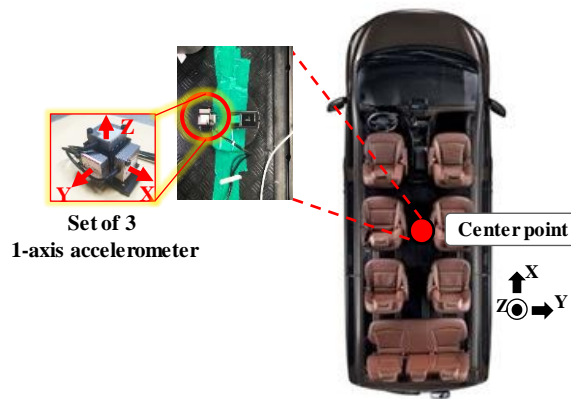
$$a_v = \sqrt{(W_{kx}^2 a_x^2 + W_{ky}^2 a_y^2 + W_{kz}^2 a_z^2)/n} \quad (3.2)$$

**Table.3. 4. Approximate indications of reactions**

<b>Magnitude of vibration(<math>a_v</math>)</b>	<b>Discomfort response</b>
0.315m/s <sup>2</sup> to 0.63m/s <sup>2</sup>	A little uncomfortable
0.8m/s <sup>2</sup> to 1.6m/s <sup>2</sup>	Uncomfortable
Greater than 2.0m/s <sup>2</sup>	Extremely uncomfortable

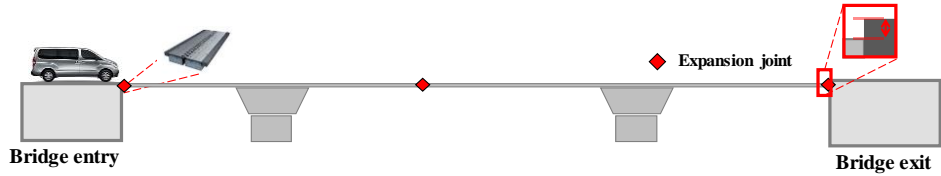
The vehicle used in the test is Hyundai's Grand Starex and three kinds of accelerometers were used for test and attached to the floor of the vehicle center. The

first accelerometer is the JOOSHIN's AC-310 1-axis analog wired accelerometer, the second accelerometer is the MicroStone MVP-SD 3-axis commercial wireless accelerometer, and the last is MPU6050 3-axis wireless accelerometer used in the proposed device. The 3-axis wired accelerometer was made by 3-axis by combining three of the 1-axis accelerometer.



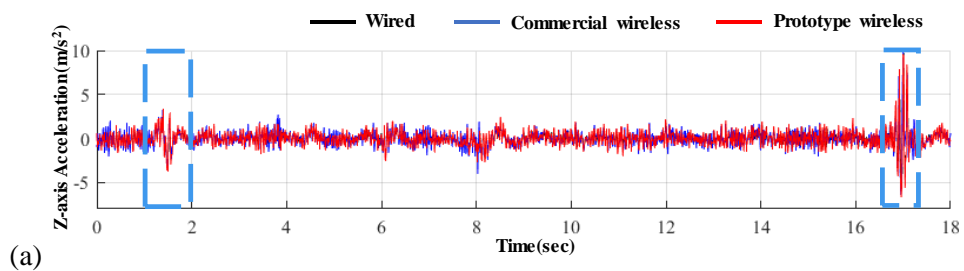
**Fig. 3. 15. Location of acceleration measuring point**

The serviceability test was conducted on the concrete bridge which has a total 400m length and there were installed the three expansion joint at both ends and the center of the bridge.



**Fig. 3. 16. . Locations of the expansion joints on the bridge**

As a result of the data measurement, it was confirmed that acceleration increases as the vehicle running speed increases. Fig.3.17 shows the vertical acceleration of the vehicle floor in time domain when driving at 100 km/h above the test bridge. Although the measured accelerations using the three accelerometers are similar in magnitude and phase, the MPU6050 is less sensitive to small acceleration variations than the MVP-SD.





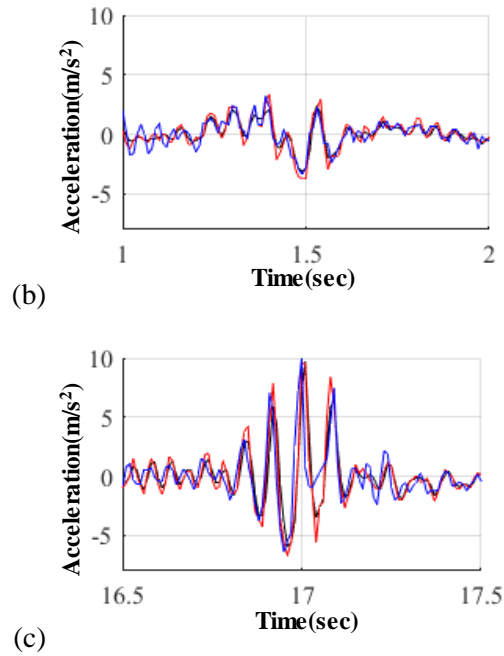


**Fig. 3. 17. Vertical acceleration of the vehicle running at 100 km/h**

Large acceleration was not measured in most sections of the bridge, but large acceleration was detected by the expansion joint and applied to the ISO serviceability evaluation. Large acceleration was not measured in most sections of the bridge, but large acceleration was detected by the expansion joint and it was calculated to the ISO serviceability.

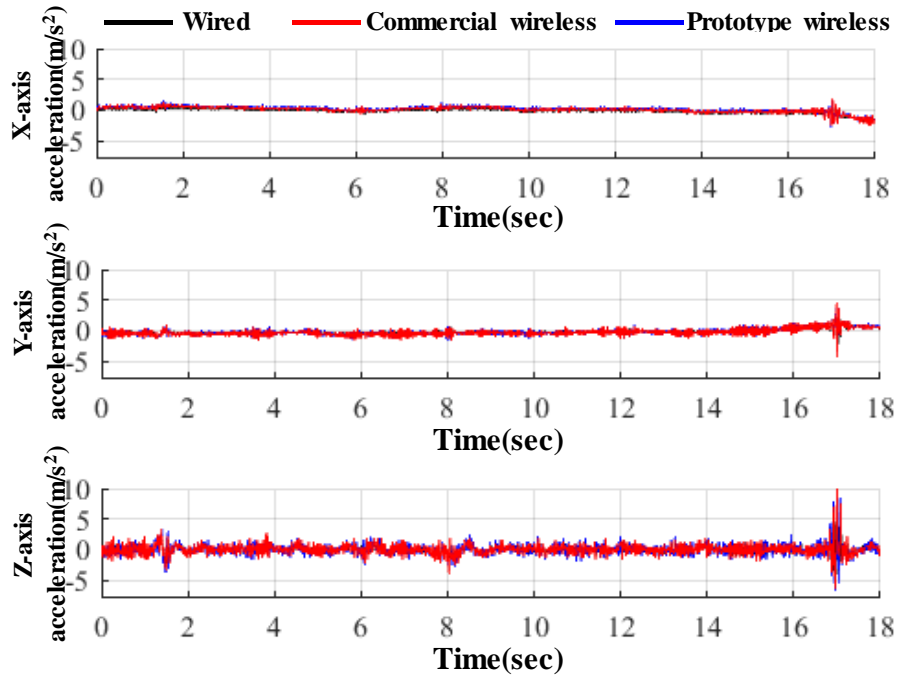


Fig. 3. 18. 3-axis of measured acceleration at 100km/h

Fig.3.18 shows the 3-axis acceleration data measured at the center of the vehicle floor running at 100 km/h, which used for evaluating serviceability.

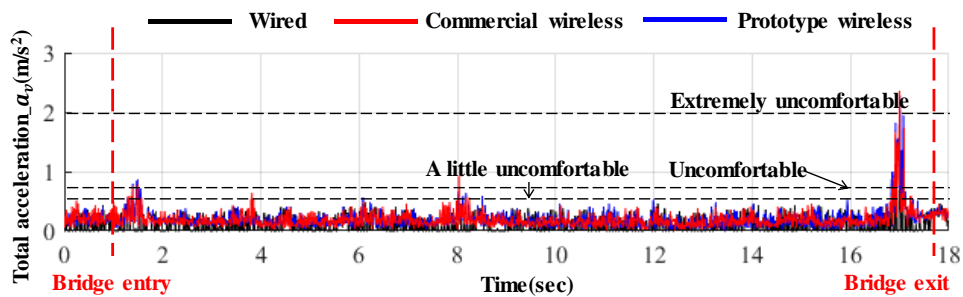


Fig. 3. 19. Total response acceleration based on ISO

Fig. 3.19 is the evaluation result of serviceability by the ISO method through the measured 3-axis acceleration data. The results show that the human body did not feel great discomfort in most of the positions of the bridge tested, but it was evaluated to feel a great inconvenience at expansion joint.

The proposed device can help to evaluate the structure and serviceability based on numerical data by easily installing the accelerometer and measuring the acceleration.

## **CHAPTER 4**

### **Pressure sensor**

#### 4.1 Type of pressure sensor

The pressure has generally measured in an environmentally controlled laboratory because the pressure value varies depending on many factors such as the shape of the structure and the temperature change. However, there is a needs to measure the actual pressure acting on the structure, as the movement due to the wind loads, such as the vibration of the bridge due to the typhoon and the vibration of the sound barrier due to the vehicle running effect.

For these reasons, the proposed device was designed for simultaneously measuring the acceleration and wind pressure of the structure to analyze wind-induced vibration.

##### 4.1.1 Piezo-resistive type pressure sensor

Piezo-resisting type pressure sensor is a device that measures pressure by using an effect that changes the resistance ratio of a crystal when external forces are applied to a semiconductor crystal.

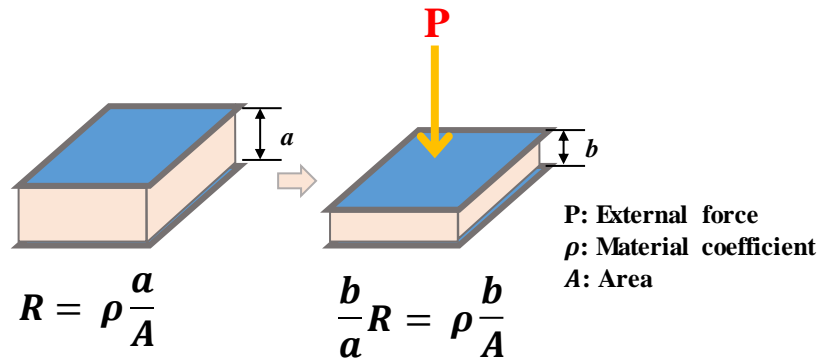


**Fig 4.1. Principle of piezo-resistive type pressure sensor**

The propose device uses Bosh’s BMP280 pressure sensor for measuring pressure. BMP280 has  $\pm 12$  Pa of accuracy and 0.16 Pa of resolution and using this pressure sensor and using this sensor, and a validation test was conducted to verify that it can measure the wind pressure acting on the structure.

## 4.2 Pressure sensor validation test

### 4.2.1 Pressure change test according to volume change in closed cylinder

A verification experiment was conducted based on the basic idea that the pressure value changes when the volume of the closed container changes

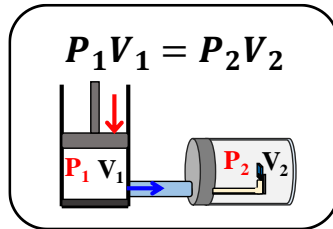


**Fig 4.2. Basic concept: Boyle's law**

As shown in Fig.4.3, BMP280 was installed in a closed container, and using the shaking table to periodically vary the volume of the inside air and measured the pressure change.

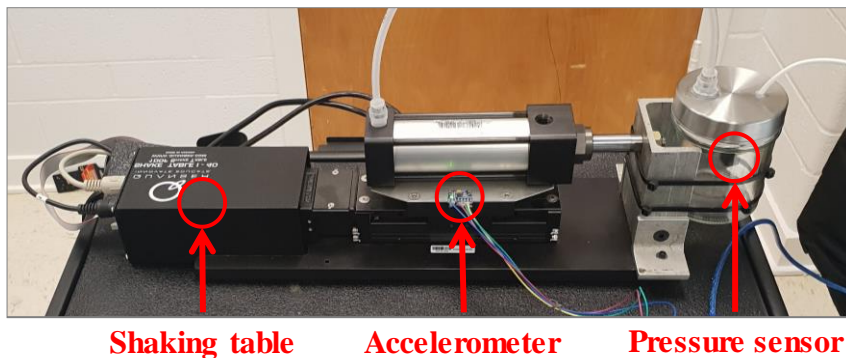


**Fig 4.3. Setup of pressure validation test using shaking table**

The experiment could not use a reference pressure sensor, so the measured pressure data through BMP280 is compared with the ideally calculated pressure through volume change. The volume change tests were carried out by varying the speed and displacement of the shaking table from 0.5 Hz to 5 Hz and from 5 mm to 20 mm. Fig.4.3 shows the pressure value that the ideally calculated pressure and

measured pressure when the shaking table moves at 2Hz and 10mm.

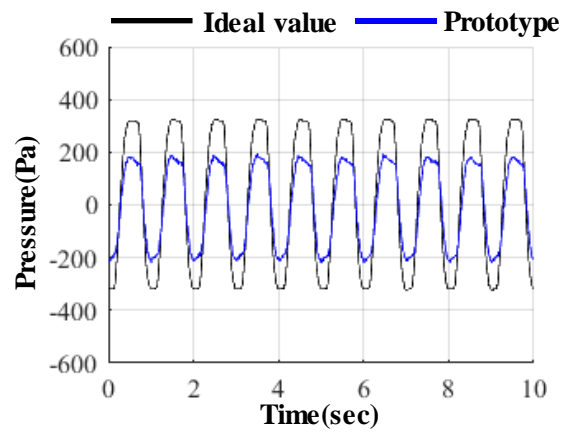


**Fig 4.4. Measured pressure data through BMP280**

Although the actual pressure value of inside the cylinder is not known due to the absence of the reference sensor, it is confirmed that the BMP280 has a constant ratio of 63% compared to the ideal calculated value.

#### 4.2.2 Pressure change test according to wind speed in wind tunnel test

The large structures, such as long-span bridges, need to know about aerodynamic properties of structure through wind tunnel tests to confirm the effects of wind. Seoul National University has a 2-dimensional wind tunnel for the structural wind resistance design, its size is  $1.0\text{m} \times 1.5\text{m}$  and can generate wind up to 20m/s.

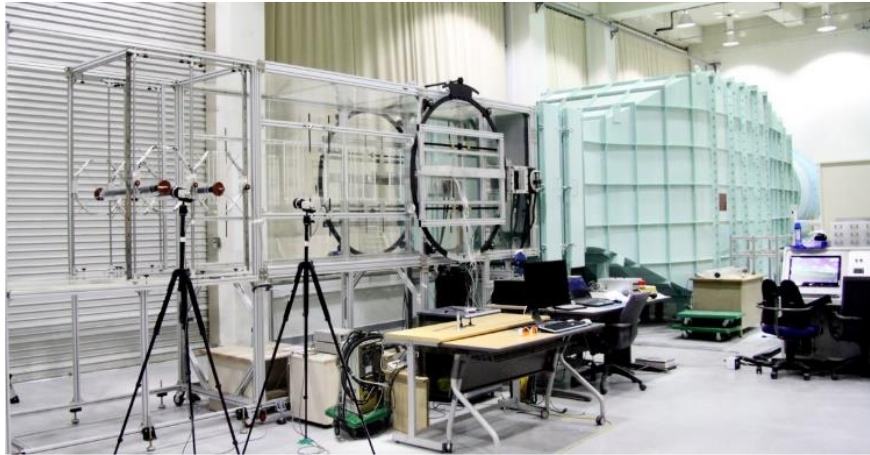


**Fig 4.5. Wind tunnel in Seoul National University**

To verify the performance of BMP280 pressure sensor used in proposed device, a wind tunnel was used to measure the wind pressure acting on the sound barrier model. The reference pressure sensor which TE connectivity's NetScanner 9116 model was used in the validation test and NetScanner9116 has 16 pressure taps, 0.21 Pa of resolution.

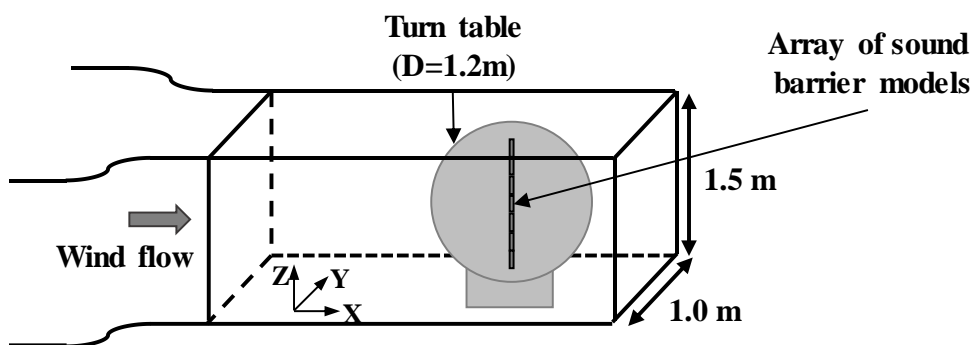


**Fig 4.6. Setup of pressure validation test using wind tunnel**



The validation tests were conducted through measuring the wind pressure acting on the sound barrier which positioned at the center of the wind tunnel. NetScanner9116 and BMP280 were attached to the same position as the sound barrier to prevent side edge effect error. The experiment condition was that vary the wind speed from 0m/s to 15m/s and measured pressure for 2 minutes.

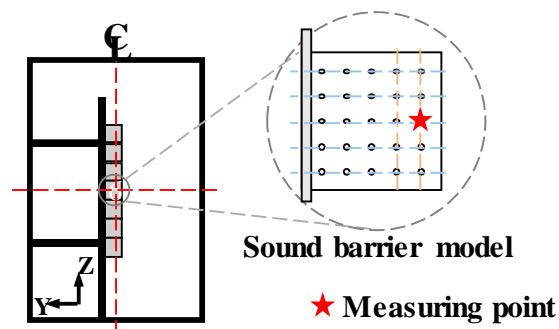


**Fig 4.7. Measuring point of sound barrier model**

Fig4.7 shows the measured pressure according to changing wind speed. The pressure of each wind speed indicated on the graph represents the average value of the pressure measured over two minutes. The graph shows that the pressure measured by the NetScanner and the pressure measured by the BMP280 are different for each wind speed.

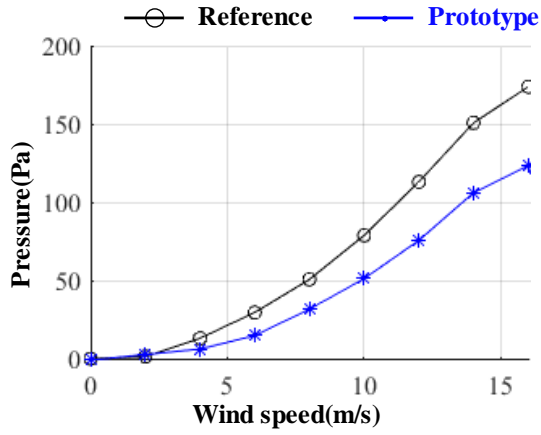


Fig 4.8. Measured pressure which acting on the sound barrier according to wind speed

Fig4.7 shows the measured pressure according to changing wind speed. The pressure of each wind speed indicated on the graph represents the average value of the pressure measured over two minutes. The graph shows that the pressure measured by the NetScanner and the pressure measured by the BMP280 are different for each wind speed.

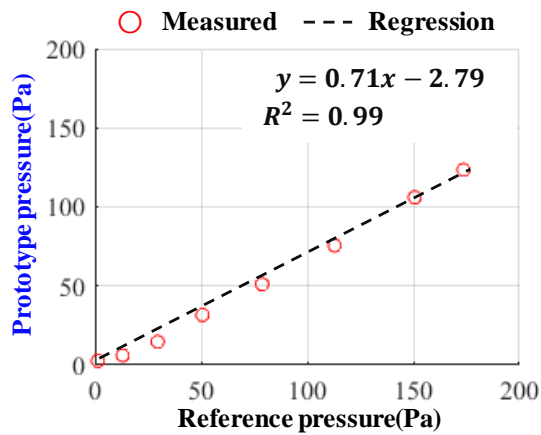


Fig 4.9. Correlation between NetScanner9116 and MPU6050

Fig4.8 has plotted the graph axis by measured data for checking the correlation between both measured data. As shown in Fig. 4.8, the graph shows that the pressure values measured at the same wind speed through both sensors have a constant ratio in all wind speed ranges.

The validation tests were carried out by measurement of pressure change due to volume change and wind speed change. Although the pressure values measured by the proposed sensor showed different with ideally calculated and measured valued through the reference sensor, both results show a constant ratio over all measurement ranges.

## **CHAPTER 5**

### **Summary and conclusions**

This study objective is development of a deployable measurement system for the civil infrastructures.

Commercial wireless devices are not free from time drift problems because they use Real Time Clock (RTC). The proposed device uses GPS to solve the time synchronization problem among devices. The GPS makes a proposed device to receive global time anywhere under the clear sky and also maintain global time through the PPS signal.

To verify the performance of the accelerometer used in the proposed device, experiments were performed using a shaking table. As a result, it was confirmed that it is less sensitive to small-high frequency vibration than the conventional wired accelerometer, but it is confirmed that the acceleration was measured in the low-frequency motion of the interest range, 0.2 Hz to 2.0 Hz. When the proposed device measured the vibration of the suspended footbridge for comparing with the conventional accelerometer in the frequency domain analysis, the maximum error was confirmed as 1.38%. Therefore, it is considered that the proposed device is applicable to measure the structural vibration.

Performance validation tests were conducted to verify that the wind pressure

can be measured using the proposed device. As a result of the validation tests, it was confirmed that the measured pressure values by the proposed device were different from the reference values, but both validation test results showed a constant correlation. Measuring wind pressure can be improved through future studies.

## REFERENCES

- [1] Rice, J. A. and Spencer Jr, B. F., (2008). "Structural health monitoring sensor development for the Imote2 platform", *Proc. SPIE Smart Structures/NDE*.
- [2] C. B. Yun, Cho, S.; Park, H.; Min, J.; Park, (2014). "J. Smart wireless sensing and assessment for civil infrastructure", *Struct. Infrastruct. Eng.* Vol.10, pp.534-550.
- [3] Cho, S., Park, J., Jung, H-J., Yun, C-B., Jang, S., Jo, H., Spencer Jr, B.F., Nagayama, T., Seo, J.W., (2010), "Structural health monitoring of cable-stayed bridge using acceleration data via wireless smart sensor network", *Bridge Maintenance, Safety, Management and Life Cycle Optimization*. pp 158-164
- [4] Jo, H., Rice, J. A., Spencer, B. F., and Nagayama, T. (2010). "Development of high-sensitivity accelerometer board for structural health monitoring," *Sensors and Smart Structures Technologies for Civil, Mechanical, Aerospace Systems*, (Bellington, WA), 764706.
- [5] Kim, R.E.; Li, J.; Spencer, B.F.; Nagayama, T.; Mechitov, K.A. (2016) "Synchronized sensing for wireless monitoring of large structures", *Smart Struct. Syst.* Vol. 18, pp.885-909.
- [6] Koo KY, Hester D and Kim S (2019) "Time Synchronization for Wireless Sensors Using Low-Cost GPS Module and Arduino". *Front. Built Environ*, Vol.4, pp.82-98.
- [7] Nagayama T, Ushita M and Fujino Y. (2011) "Suspension bridge vibration measurement using multihop wireless sensor networks". *Proc Eng*, Vol.14, pp.761-768..
- [8] R. Kim, T. Nagayama, H. Jo, J. Spencer, (2012) "Preliminary study of low-cost GPS receivers for time synchronization of wireless sensors", *Proc. SPIE Sensors Smart Struct. Technol. Civ. Mech. Aerosp. Syst.*, Vol. 8345, no. 1, pp. 83451A-83451A,
- [9] R. Shaladi, F. Alatshan, C. Yang, (2015) "An overview on the applications of structural health monitoring using wireless sensor networks in bridge engineering", *Proc. Int. Conf. Adv. Sci. Eng. Technol. Nat. Resources*, pp. 4-11.

- [10] S. Youn, (2013) "A Comparison of Clock Synchronization in Wireless Sensor Networks", *Int. J. Distrib. Sens. Networks*, Vol. 2013, pp. 10.
- [11] Y. Marjanen, (2010) "Validation and improvement of the ISO 2631-1(1997) standard method for evaluating discomfort from whole-body vibration in a multi-axis environment", PhD thesis, Loughborough University.

## 국 문 초 록

본 연구에서는 토목 인프라 구조물의 동적 특성을 계측하기 위한 설치 편의형 계측 시스템 개발에 대한 연구를 수행하였다.

이론적 유체역학이 지속적으로 발전되었고 유체의 흐름을 해석하는 방법들이 빠르게 개발되었지만, 장대교량과 고층빌딩, 방풍벽 등과 같이 바람의 영향으로 진동이 크게 발생하는 인프라 구조물들은 실제 움직임을 계측하여 동적 특성을 분석하는 것이 필수적이다.

현재 계측 시스템은 발전기와 데이터 저장장치, 센서, 케이블 등 많은 장비가 필요하기 때문에 이를 운영 중인 교량과 고층빌딩에 설치하여 계측하는 과정에 많은 어려움이 있다. 이와 같은 문제를 해결하기 위해 전원과 데이터 저장장치, 센서가 일체화된 무선 계측 장치를 개발할 필요가 있으며, 이는 연구자와 공학자들이 인프라 구조물 운영에 영향을 주지 않으면서 원하는 지점에서 구조물의 진동을 계측하는 것에 도움을 줄 것이다.

이 연구에서는 GPS를 이용하여 기기간 시간 동기화를 유지하고, MEMS 가속도 센서 및 MEMS 압력 센서를 활용하여 구조물의 진동과 구조물에 작용하는 압력을 계측하는 설치 편의형 계측 장치를 제안한다.



주요어: 구조물 계측 시스템, MEMS 센서, 구조물 진동, 무선 계측장치,

GPS기반 시간 동기화

학번: 2017-27232